Thermally Anisotropic Composites for Heat Redirection and Thermal Management in Building Envelopes

Kaushik Biswas, PhD **Som Shrestha, PhD, BEMP** **Diana Hun, PhD**
Member ASHRAE

Jerald Atchley

ABSTRACT HEADING

In building envelope systems, thermal management is important from energy conservation and thermal comfort perspectives, and is typically done via insulation, thermal mass, solar control and shading, etc. Thermal anisotropy is commonly utilized in electronics for heat dissipation. This article investigates the feasibility of utilizing thermally anisotropic composites (TACs) to reduce unwanted heat gains and losses through the building envelope by redirecting the heat transfer to or from appropriate heat sinks and sources.

Numerical simulations of building envelope components using finite element analysis (FEA) and whole building simulations using EnergyPlus (E+) were performed to estimate the energy savings potential of TACs used in external walls of residential buildings. Application of TACs was compared with baseline walls with cavity insulation as well as with and without exterior continuous insulation (CI). The (FEA) simulations indicated 75% or higher reductions in heat gains when using a TAC coupled with a heat sink compared to an exterior CI case. In terms of energy savings in a hot climate, E+ models estimated cooling energy savings of 19% with a "TAC + heat sink" compared to a baseline wall with only cavity insulation. Further, a small-scale test sample with a TAC-heat sink system was built and tested in a multi-transducer heat flow meter apparatus (HFMA). The heat sink was a copper tube circulating cold water. The experiments verified the re-direction of heat to a sink and significant reduction in heat transfer through the test specimen. The experiments showed that the heat redirection only occurred in the presence of both thermal anisotropy and water circulation; if either element was missing, the system behaved like a traditional envelope component.

INTRODUCTION

In building envelope systems, thermal management is important from energy conservation and thermal comfort perspectives. Thermal management to reduce or eliminate unwanted heat flows through the opaque building envelope sections (walls, roof and foundation) has traditionally been done via insulation, thermal mass, solar control and shading, etc. (Sadineni et al. 2011, Santamouris et al. 2007). Recent advances in roofs include green roofs, photovoltaic roofs, radiant-transmittive barriers, evaporative roof cooling systems, above-sheathing-ventilation and phase change materials (PCM) (Sadineni et al. 2011, Kosny et al. 2012, and references therein). PCMs have also shown the potential for large reductions in wall-generated heating and cooling loads (Biswas and Abhari 2014, Biswas et al. 2014). Vacuum insulation panels (VIPs) and aerogels are among the new generation of high-performance insulation materials being investigated for building envelope applications (Baetens et al. 2010, Baetens et al. 2011); these can provide similar higher thermal resistance compared to current building foam and fibrous insulation materials. Current building

Kaushik Biswas and **Som Shrestha** are R&D Staff, **Diana Hun** is a sub-program manager and R&D Staff, and **Jerald Atchley** is a Master Technician at Oak Ridge National Laboratory, Oak Ridge, TN.

insulation materials (fiberglass and foam) have thermal conductivities in the 0.024 – 0.039 W/m-K (0.17-0.27 Btu-inch/h-ft^2-°F) range; aerogel and VIP have nominal conductivities of 0.012 and 0.004 W/m-K (0.083 and 0.028 Btu-inch/h-ft^2-°F), respectively.

This study investigates the feasibility of applying thermally anisotropic materials (TAMs) and composites for active thermal management in building envelopes. TAMs have been applied for improved heat dissipation and hot spot remediation in electronics (Bachmann and Bar-Cohen 2008, Suszko and El-Genk 2016, El-Genk and Ali 2013, Huang et al. 2016). A series of two-dimensional (2D) numerical simulations were performed using a finite element analysis (FEA) tool of TACs applied to a wall cross-section to determine the potential reductions in unwanted heat gains and losses through walls. The TACs consisted of alternate layers of regular foam insulation and a high-conductivity material (for example, aluminum). Next, the 2D simulations of a wall cross-section were combined with whole building models using EnergyPlus (E+). The E+ simulations were used to estimate energy savings for the whole-building based on the calculated wall-generated heating and cooling loads from the 2D models. Finally, a small-scale prototype of the TAC was created and tested in a custom heat flow meter apparatus (HFMA). HFMA are typically used to measure thermal transmission properties of homogeneous building materials according to ASTM C518 (2017). The custom HFMA contains multiple transducers that can map the heat flow distribution through inhomogeneous samples.

SIMULATION METHODOLOGY AND PARAMETERS

Figure 1 shows the model geometries used in the 2D FEA simulations. The geometries show horizontal cross-sections of the modeled walls, extending from the centerline of a cavity to the centerline of a neighboring wood stud. For these initial simulations, the baseline wall consisted of a 2x4 wood-framed wall with cavity and exterior continuous insulation (CI). The cavity insulation was assumed to be fiberglass batt and the exterior CI was 5.1 cm (2 inch) of polyisocyanurate (PIR). The TAC case was same as the baseline wall, except the exterior CI was replaced with a TAC consisting of four pairs of alternating 1.3 cm (0.5 inch) PIR and aluminum (Al) foil. The material properties were taken from commonly available literature for building materials, such as the ASHRAE Handbook of Fundamentals.[1] The exterior boundary condition was based on radiative and convective heat exchange with the outside, following Biswas et al. (2014). The interior boundary condition assumed a heat transfer coefficient of 8.29 W/m^2-K (1.46 Btu/ft^2-h-°F) for a non-reflective vertical surface and the interior (room) temperature was allowed to float between assumed heating and cooling set points (Biswas et al. 2014). The heat sink was assumed to be at a temperature lower than the outdoor temperature by a specified amount. Assuming symmetry, only a small portion of the wall spanning the middle of a cavity and the middle of a stud was modeled.

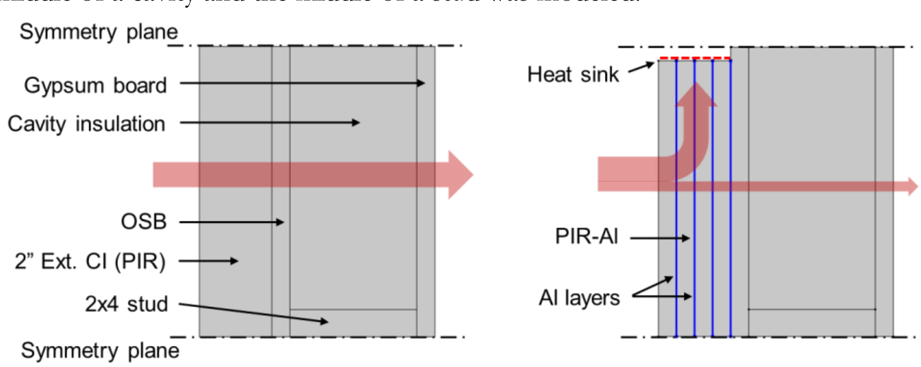

Figure 1 Modeled baseline wall (left) and wall with TAC and a heat sink (right).

Figure 1 also includes thick arrows depicting the expected impact of the TAC-heat sink combination. Under

[1] https://www.ashrae.org/technical-resources/ashrae-handbook/description-2017-ashrae-handbook-fundamentals

summer conditions, the thick arrow on the left represents the heat transfer through a baseline wall while the diverging arrows on the right indicate that the high-conductivity Al layers connected to a heat sink divert a major portion of the heat away from the interior space.

The next step was to build an E+ baseline whole building model, based on a residential prototype building model developed for the Department of Energy (DOE) Building Energy Codes Program.[2] The building used for this study was a wood-framed, two-story single-family detached house with a total conditioned floor area of about 177 m^2 (1900 ft^2) and compliant with International Energy Conservation Code (IECC) (2006). It is noted that a major portion of residential buildings in the US are older and not insulated up to IECC 2006 levels; however, this is the earliest vintage available in the set of prototype building models. Table 1 lists the details of the baseline wall construction and the relevant thermo-physical properties of the wall components in the E+ model. The properties listed for the cavity layer are effective weight-averaged properties accounting for the joint impact of the cavity insulation and wood studs.

Table 1. Details And Relevant Material Properties of Exterior Walls of The Baseline Building

	Thickness cm (inch)	Conductivity W/m-K (Btu-inch/h-ft^2-°F)	R-value m^2-K/W (h-ft^2-°F/Btu)	Density kg/m^3 (lb/ft^3)	Specific Heat kJ/kg-K (Btu/lb-°F)
Stucco	0.64 (0.25)	1.40 (9.70)	0.005 (0.03)	1920.0 (120.0)	0.88 (0.21)
Sheathing	1.3 (0.5)	0.09 (0.65)	0.135 (0.77)	684.2 (42.8)	1.17 (0.28)
Oriented strand board (OSB)	1.6 (0.6)	0.12 (0.80)	0.137 (0.78)	544.0 (34.0)	1.21 (0.29)
Cavity layer	8.9 (3.5)	0.06 (0.42)	1.490 (8.46)	120.7(7.5)	1.04 (0.25)
Drywall	1.3 (0.5)	0.16 (1.11)	0.079 (0.45)	800.0 (50.0)	1.09 (0.26)

To capture the impact of the TACs, a new approach was taken to couple the FEA and E+ models. The process started with a baseline whole-building E+ simulation to generate the indoor and outdoor boundary conditions for the 2D FEA models. Next, the FEA models calculated the wall-generated heating and cooling loads from the baseline, 'baseline + exterior insulation' and 'baseline + TAC' wall configurations. Finally, another set of E+ simulations were performed using the FEA-calculated hourly heat gains and losses through the exterior walls as inputs. Since E+ assumes one-dimensional heat transfer through exterior walls, it cannot capture 2D heat transfer effects. Also, there is no direct method in E+ to model a building envelope system that is connected to a heat sink or source. Therefore, a modified E+ simulation methodolgy was developed. In all cases, the opaque sections of the exterior walls in the E+ models were converted to adiabatic surfaces. The FEA-calculated heat gains and losses through the exterior walls were modeled as internal heating and cooling loads using the 'OtherEquipment' option in E+. The windows and exterior doors were split into separate sections from the opaque wall sections and treated normally in the E+ models. This was necessary as a section of a wall containing a door or window cannot be modeled as an adiabatic surface. The energy consumption by the HVAC equipment were calculated for the cases with exterior insulation and TAC, and compared against the baseline.

The baseline building was modeled using typical meteorological year (TMY)[3] weather data for Phoenix, AZ and Baltimore, MD. Phoenix falls under climate zone 2 (hot, cooling-dominated) and Baltimore is in zone 4 (mixed, needing cooling and heating). The results of the baseline model were used for comparison against results of building models implementing exterior continuous insulation (CI) or TAC. The weather inputs and calculated indoor temperatures of the E+ baseline model were also used as inputs for the 2D wall model. The material properties for the FEA models were the same as in the E+ baseline model, except for the cavity insulation, stud and the exterior layers not used in the E+ baseline model. The FEA model required separate sets of properties for the cavity insulation

[2] https://www.energycodes.gov/development/residential/iecc_models

[3] http://rredc.nrel.gov/solar/old_data/nsrdb/1991-2005/tmy3/

and studs, unlike the E+ model that used a single set of effective properties that combined their effects. Table 2 lists the additional materials properties used in the FEA simulations.

Table 2. Additional material properties used in the FEA simulations

	Thickness cm (inch)	Conductivity W/m-K (Btu-inch/h-ft^2-°F)	Density kg/m^3 (lb/ft^3)	Specific Heat kJ/kg-K (Btu/lb-°F)
Cavity insulation	8.9 (3.5)	0.054 (0.37)	73.6 (4.6)	0.60 (0.14)
2x4 stud[4]	8.9 (3.5)	0.115 (0.80)	576 (36.0)	1.63 (0.39)
PIR (1)	3.8 (1.5)	0.024 (0.17)	32 (2.0)	1.45 (0.35)
PIR (2)	1.3 (0.5)	0.024 (0.17)	32 (2.0)	1.45 (0.35)
Al	0.01 (0.005)	238 (1650.2)	N.A.	N.A.

EXPERIMENTAL METHODOLOGY

For experimental verification of the anisotropic concept, some small-scale tests were done in a HFMA. Figure 2 shows the TAC-heat sink configuration. The TAC consisted of three alternating layers of Al foil and 0.6 cm (0.25 inch) extruded polystyrene (XPS) foam sheets. The TAC was sandwiched by 1.3 cm (0.5 inch) gypsum sheets. The Al foils were connected to a copper tube with cold water circulation to act as the heat sink. The entire assembly was placed within the HFMA, whose upper and lower plates can be maintained at different temperatures, and the heat flows through the test specimen can be measured.

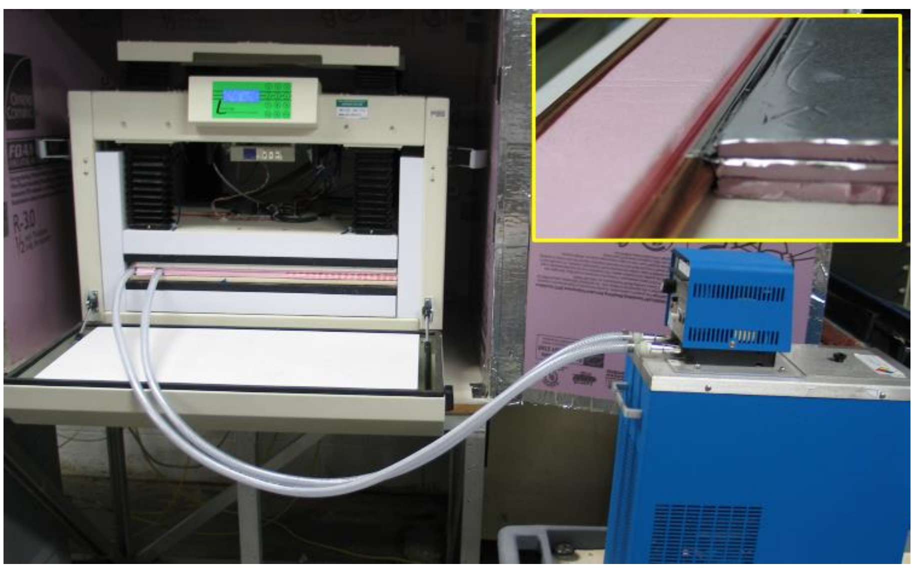

Figure 2 Small-scale anisotropic sample in an HFMA; Inset – TAC consisting of alternating layers of XPS sheet and Al foil (3 each) connected to a copper tube with circulating water acting as the heat sink.

Two tests were performed, the first with the Al foil layers and the second test was done after removing the Al foil layers. The HFMA contains an array fifteen heat flux transducers (HFTs) in each plate to measure the heat flows through different regions of tested samples. Figure 3 shows the relative locations of HFTs 5-8 in the HFMA plates with respect to the TAC and the copper tube. The tests were run for multiple hours and the water circulation was turned on and off during the test periods.

[4] Thermal conductivity obtained from http://www.coloradoenergy.org/procorner/stuff/r-values.htm

Figure 3 Relative locations of HFTs with respect to the copper tube.

RESULTS AND DISCUSSIONS

2D FEA Simulations

Figure 4 compares snapshots of FEA-calculated temperature distributions within the baseline and TAC walls under summer conditions in Phoenix, AZ. The walls were assumed to be west facing. The TAC consisted of four layers of 1.3 cm (0.5 inch) PIR and Al foils, the heat sink temperature was assumed to be 10°C (18°F) lower than the outdoor temperatures and the heat transfer coefficient at the TAC-heat sink interface was assumed to be 10 W/m^2-K (1.76 Btu/ft^2-h-°F). The temperature distributions in figure 4 indicate the effectiveness of the TAC-heat sink system in reducing the depth of penetration of the external heat and, consequently, reducing the interior heat gains.

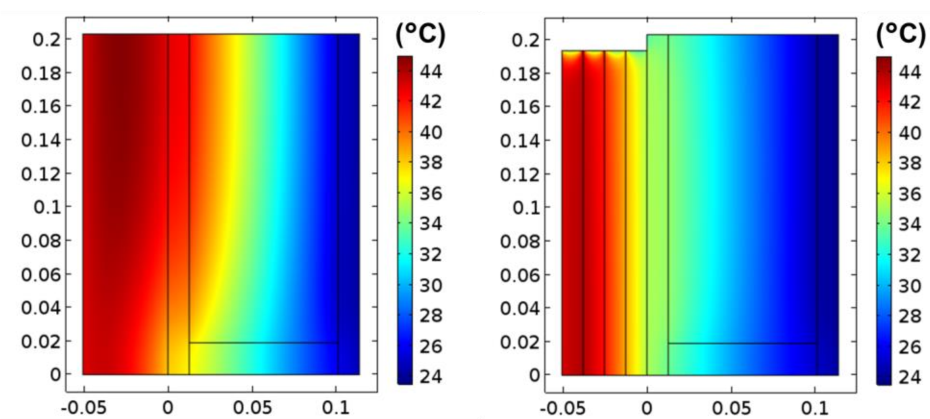

Figure 4 Snapshots of temperature distributions within the baseline wall (left) and TAC wall (right) under summer conditions.

Figure 5 compares the monthly integrated heat flows into the interior space from the two walls. The interior heating and cooling set points were assumed to 20 and 23.3°C (68 and 73.9 °F), respectively. Under the current assumptions, on an annual basis, the TAC wall reduced the internal heat gains by 69%. Further parametric simulations were performed by varying different parameters: heat transfer coefficient at the heat sink, temperature difference between the heat sink and outside, thickness of Al layers, and the number of Al layers (two and four). The most significant impacts on the TAC performance were observed with the heat sink temperature, followed by the heat transfer coefficient. Lowering the heat sink temperature by 20°C (36°F) below the outdoor temperature eliminated all interior heat gain. Varying the heat transfer coefficient from 5 to 50 W/m²-K (0.88-8.81 Btu/ft²-h-°F) reduced the interior heat gains by 59 to 81% compared to the baseline, but further increase in heat transfer coefficient didn't have a big impact. Even with just two layers of PIR-Al, similar annual heat gain reductions were observed as four layers.

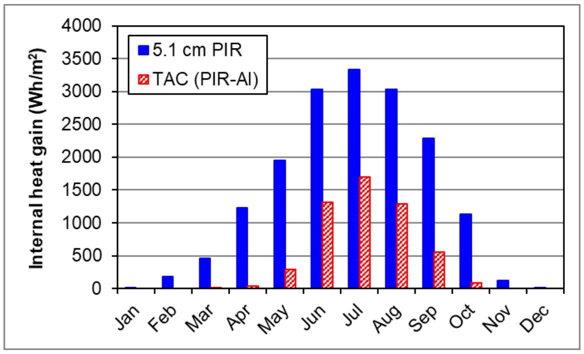

Figure 5 Comparison of monthly integrated heat gains.

Coupled FEA-E+ Simulations

The following cases were modeled for the coupled FEA and E+ simulations and analyses:

1. Baseline – baseline wall configuration from the original residential prototype building model.
2. Ext. CI – 3.8 cm (1.5 inch) PIR as added exterior CI to the baseline wall.
3. PIR-Al(1) – anisotropic composite consisting of three layers of 1.3 cm (0.5 inch) Al foil-faced PIR added to the baseline wall and coupled with a heat sink that was always assumed to be 10°C (18°F) lower than the outside ambient temperature.
4. PIR-Al(2) – similar to PIR-Al(1), except the heat sink was turned off when the outside temperature was below 12.78°C (55°F). 12.78°C (55°F) is often assumed as the balance point for buildings, i.e., the temperature below which buildings would require heating.
5. PIR-Al(3) – similar to PIR-Al(1), but the heat sink temperature was 10°C lower than outside temperature when the outside temperature was higher than 12.78°C; when the outside temperature was lower than 12.78°C (55°F), the heat sink was switched to a heat source with temperatures 10°C (18°F) higher than the outside temperature. This case was only simulated for Baltimore weather, where the heating requirement is usually higher than Phoenix.

Table 1 lists the analysis results in terms of electricity consumption for cooling and natural gas consumption for heating. In general, the TAC scenarios performed significantly better than the ext. CI for reducing electricity use. With a constant 10°C (18°F) difference between the outdoor and heat sink temperatures, the anisotropic composites resulted in a heating penalty compared to the baseline case. By turning off the heat sink at 12.78°C (55°F), modest heating gains of 4.7-4.8% were estimated with respect to the baseline case. The PIR-Al(3) case, which switched between heat sink and heat source when the outdoor temperature was above or below 12.78°C (55°F), both significant cooling and heating energy savings were estimated; the cooling energy savings were similar to the other anisotropic composite-heat sink scenarios while the heating energy savings were close to the ext. CI case.

Based on the current analyses results, using anisotropic composites coupled with suitable heat sinks and sources has the potential for significant reductions in heating and cooling energy consumption in residential buildings. The cooling energy savings from TACs under Phoenix-like weather conditions can be twice as much as the savings achieved by an exterior CI layer of the same thickness. In fact, another set of simulations performed using a 1.9 cm (0.75 inch) thick TAC under Phoenix weather conditions estimated a cooling energy reduction of 14.2%, higher than the 11.7% reduction achieved by the 3.8 cm (1.5 inch) exterior CI.

Table 3. Comparison of Calculated Energy Consumption For Cooling And Heating in Phoenix And Baltimore

	Electricity kWh	% difference	Natural gas Therm	% difference
		Phoenix		
Baseline	11608.5		149.8	
Ext. CI	10252.2	-11.7%	111.8	-25.4%
PIR-Al (1)	9368.1	-19.3%	156.6	4.5%
PIR-Al (2)	9384.1	-19.2%	142.8	-4.7%
		Baltimore		
Baseline	4262.7		749.6	
Ext. CI	3777.6	-11.4%	640.8	-14.5%
PIR-Al (1)	3191.4	-25.1%	773.3	3.2%
PIR-Al (2)	3176.3	-25.5%	713.8	-4.8%
PIR-Al (3)	3162.6	-25.8%	655.2	-12.6%

As described in the previous sub-section, the heat sink and source temperatures have a big impact on the efficacy of the TAC system. One possibility for heat sinks and sources is to couple the TACs with the ground via pipes with coolant flow, heat pipes, etc. Xing and co-workers (Xing and Spitler 2016a, Xing and Spitler 2016b, Xing et al. 2016) developed an analytical model to predict undisturbed ground temperatures at different depths. Based on the work of Xing and co-workers, temperatures at 3 m (9.8 ft) below the ground were calculated to be ≥15 K (22.5°R) higher or lower than the ambient winter and summer time temperatures in the Phoenix and Baltimore. Thus, the use of the ground as heat sink or source for reducing summer time heat gains and winter time heat losses appears promising.

Proof-of-concept Experimental Testing

In the HFMA tests, the upper plate was set at 40°C (104°F), the lower plate was set at 10°C (50°F) and the circulating water chiller temperature was 5°C (41°F). Figure 7 shows the temporal evolution of the measured heat flows by HFTs 6-8 in the top plate. The timing and duration of the water circulation being turned on and off are also shown. The impact of turning the water circulation on and off on the measured heat flows are clearly observable. When the water circulation was turned on, the copper tube acted as a heat sink providing directional heat dissipation due to the high thermal conductivity of the Al foil layers connected to the tube. The heat flow in the upper plate increased when the water circulation was turned on to compensate for heat removal by the circulating water and maintain the plate temperature at 40°C (104°F). Also noticeable is the impact on the HFTs based on their location. The magnitude of the change in heat flow progressively decreased with the distance of the HFT from the copper tube (i.e. HFT 6 > 7 > 8). Another test was performed by removing the Al foils. Figure 8 shows the measured heat fluxes without the Al foils with the water circulation turned on and off. Unlike the case with the Al foils, significant changes in the measured heat fluxes were not observed. Thus, the HFMA tests showed that directional heat dissipation can be achieved with a combination of a TAC and a heat sink, but both thermal anisotropy and a heat sink (or source) are required.

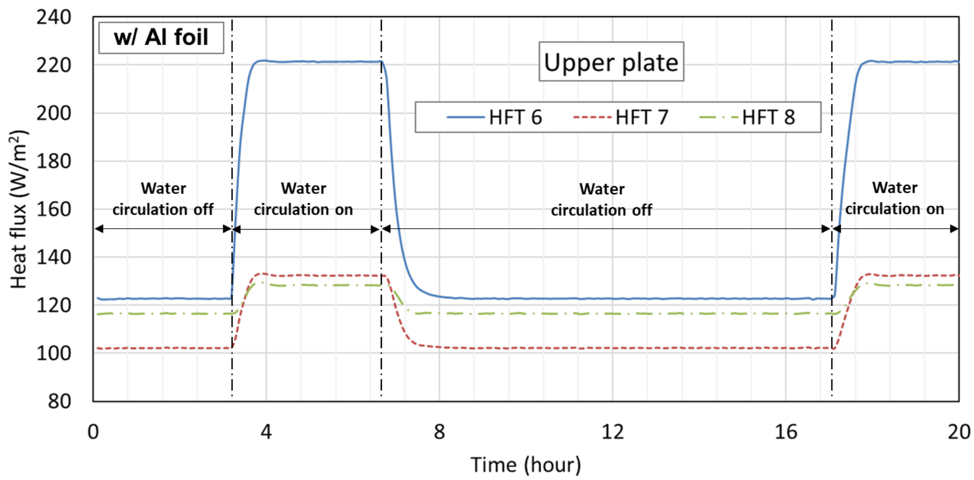

Figure 7 Heat flow measurements from the upper plate HFTs from the test with the Al foil layers.

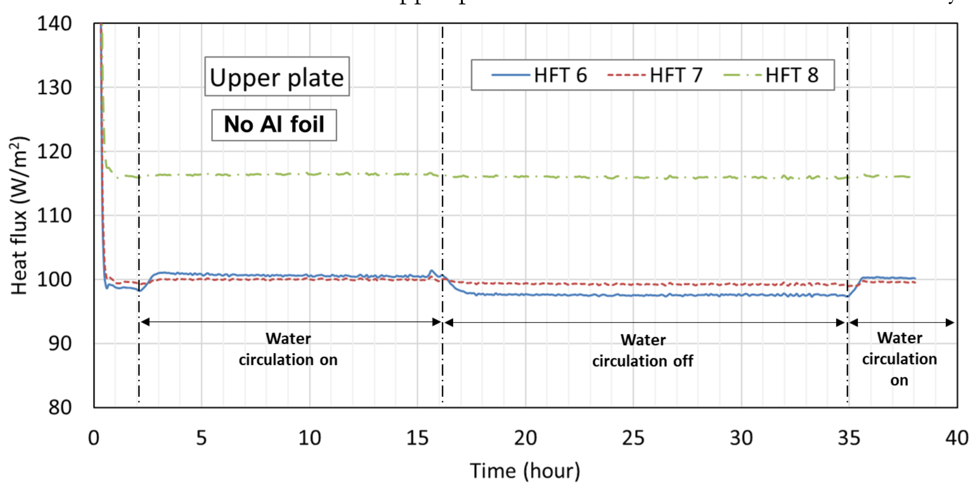

Figure 8 Heat flow measurements from the upper plate HFTs from the test without the Al foil layers.

SUMMARY

In summary, the application of thermally anisotropic composites coupled with a heat sink/source has the potential for significant reductions in envelope-generated heating and cooling loads in buildings. Combined FEA and EnergyPlus simulations of a typical two-story, single-family residential building, predicted annual savings of 19-26% in cooling energy use and 13-26% in heating energy use under Phoenix and Baltimore weather conditions. In the cases considered, the anisotropic composite consisted of three layers of aluminum foil-faced polyisocyanurate foam boards. It is noted that the baseline building chosen for modeling was IECC 2006 compliant. A major fraction of residential buildings in the US are older and are expected to have lower insulation levels than the IECC 2006 requirement. Therefore, the current analysis can be considered conservative in terms of estimates of energy savings. Further, experimental proof-of-concept of the TAC-heat sink concept was demonstrated by small-scale tests in a heat flow meter.

ACKNOWLEDGMENTS

This work was supported by the Building Technologies Office of the U. S. Department of Energy under Contract No. DE-AC05-00OR22725 with UT-Battelle, LLC. The authors would like to thank the DOE's Mr. Sven Mumme for his support of this project.

REFERENCES

ASTM C518-17, Standard Test Method for Steady-State Thermal Transmission Properties by Means of the Heat Flow Meter Apparatus, ASTM International, West Conshohocken, PA, 2017, www.astm.org.

Bachmann, C., & Bar-Cohen, A. (2008, May). Hotspot remediation with anisotropic thermal interface materials. In Thermal and Thermomechanical Phenomena in Electronic Systems, 2008. ITHERM 2008. 11th Intersociety Conference on (pp. 238-247). IEEE.

Baetens, R., Jelle, B. P., Thue, J. V., Tenpierik, M. J., Grynning, S., Uvsløkk, S., & Gustavsen, A. (2010). Vacuum insulation panels for building applications: A review and beyond. Energy and Buildings, 42(2), 147-172.

Baetens, R., Jelle, B. P., & Gustavsen, A. (2011). Aerogel insulation for building applications: a state-of-the-art review. Energy and Buildings, 43(4), 761-769.

Biswas, K., & Abhari, R. (2014). Low-cost phase change material as an energy storage medium in building envelopes: experimental and numerical analyses. Energy Conversion and Management, 88, 1020-1031.

Biswas, K., Lu, J., Soroushian, P., & Shrestha, S. (2014). Combined experimental and numerical evaluation of a prototype nano-PCM enhanced wallboard. Applied Energy, 131, 517-529.

El-Genk, M., & Ali, A. (2013). Advanced spreaders for enhanced cooling of high power chips. Frontiers in Heat and Mass Transfer (FHMT), 3(4).

Huang, S., Bao, J., Ye, H., Wang, N., Yuan, G., Ke, W., Zhang, D., Yue, W., Fu, Y., Ye, L. & Jeppson, K. (2016, August). The effects of graphene-based films as heat spreaders for thermal management in electronic packaging. In Electronic Packaging Technology (ICEPT), 2016 17th International Conference on (pp. 889-892). IEEE.

International Energy Conservation Code, 2006. http://shop.iccsafe.org/codes/other-codes/2006-international-codes/2006-international-energy-conservation-coder-pdf-download.html.

Kośny, J., Biswas, K., Miller, W., & Kriner, S. (2012). Field thermal performance of naturally ventilated solar roof with PCM heat sink. Solar Energy, 86(9), 2504-2514.

Sadineni, S. B., Madala, S., & Boehm, R. F. (2011). Passive building energy savings: A review of building envelope components. Renewable and Sustainable Energy Reviews, 15(8), 3617-3631.

Santamouris, M., Pavlou, K., Synnefa, A., Niachou, K., & Kolokotsa, D. (2007). Recent progress on passive cooling techniques: Advanced technological developments to improve survivability levels in low-income households. Energy and Buildings, 39(7), 859-866.

Suszko, A., & El-Genk, M. S. (2016). Thermally anisotropic composite heat spreaders for enhanced thermal management of high-performance microprocessors. International Journal of Thermal Sciences, 100, 213-228.

Xing, L., & Spitler, J.D. (2016a). Prediction of undisturbed ground temperature using analytical and numerical modeling. Part I: Model development and experimental validation. Science and Technology for the Built Environment, DOI: 10.1080/23744731.2016.1258371.

Xing, L., & Spitler, J.D. (2016b). Prediction of undisturbed ground temperature using analytical and numerical modeling. Part II: Methodology for developing a world-wide dataset. Science and Technology for the Built Environment, DOI: 10.1080/23744731.2016.1262705.

Xing, L., Spitler, J.D., & Bandyopadhyay, A. (2016). Prediction of undisturbed ground temperature using analytical and numerical modeling. Part I: Model development and experimental validation. Science and Technology for the Built Environment, DOI: 10.1080/23744731.2016.1258371.